

Electron transport in nodal-line semimetals

S. V. Syzranov^{1,2,3} and B. Skinner⁴

¹*Joint Quantum Institute, NIST/University of Maryland, College Park, Maryland 20742, USA*

²*School of Physics and Astronomy, Monash University, Victoria 3800, Australia*

³*Physics Department, University of California, Santa Cruz, California 95060, USA*

⁴*Massachusetts Institute of Technology, Cambridge, Massachusetts 02139, USA*

(Received 8 January 2017; revised manuscript received 12 May 2017; published 11 October 2017)

We study the electrical conductivity in a nodal-line semimetal with charged impurities. The screening of the Coulomb potential in this system is qualitatively different from what is found in conventional metals or semiconductors, with the screened potential ϕ decaying as $\phi \propto 1/r^2$ over a wide interval of distances r . This unusual screening gives rise to a rich variety of conduction regimes as a function of temperature, doping level, and impurity concentration. In particular, nodal-line semimetals exhibit a diverging mobility $\propto 1/|\mu|$ in the limit of vanishing chemical potential μ , a linearly increasing dependence of the conductivity on temperature, $\sigma \propto T$, and a large weak-localization correction with a strongly anisotropic dependence on magnetic field.

DOI: [10.1103/PhysRevB.96.161105](https://doi.org/10.1103/PhysRevB.96.161105)

Introduction. A topological semimetal is a semimetal in which the conduction and valence bands touch at a point or a line (the nodal line) in momentum space. The most well-known examples are Weyl [1–6], nodal-line [7,8], and parabolic [9] semimetals. Such materials have been in the focus of researchers' attention since their discovery several years ago, owing to the abundance of novel fundamental phenomena predicted in them, including the chiral anomaly [10], topologically protected Fermi arcs [1,3,6], and unconventional disorder-driven transitions [11].¹

In the presence of disorder, topological semimetals may display a rich variety of electrical conduction regimes, depending on the nature of quenched disorder, temperature, and doping level. For example, these systems may exhibit metallic or insulating transport properties or unconventional dependencies of the conductivity on temperature. In general, transport in topological semimetals is determined by the behavior of several potentially competing factors at energies near the band touching, including the vanishing density of states (in the disorder-free limit), divergence of the screening length, and the behavior of the elastic scattering rate.

Although the conductivity of Weyl semimetals has received considerable attention in the literature, other types of semimetals have largely evaded researchers' attention. In this paper we study the conductivity of a three-dimensional (3D) nodal-line semimetal (NLS), where the conduction and valence bands touch along a line in momentum space, as in the recently discovered ZrSiS [7], HfSiS [12], and PbTaSe₂ [8] (a number of other materials have also been predicted to be NLSs [13–20]). We calculate the NLS conductivity microscopically and study its dependence on temperature, doping level, and impurity concentration for realistically achievable regimes. We demonstrate that the Coulomb interaction in a low-doped NLS is only partially screened and has the distance dependence $\propto 1/r^2$ across a broad interval of r , which leads to qualitatively new features in conduction and a richer variety of transport regimes as compared to other semimetals, semiconductors,

and metals. In particular, NLSs display divergent quasiparticle mobility in the limit of vanishing doping, linear dependence of conductivity on temperature, and large weak-localization corrections to the conductivity with a strongly anisotropic dependence on magnetic field.

Model. It may be assumed normally that in an undoped NLS all points of the nodal line lie at the Fermi energy. In a doped material, where a finite carrier concentration is provided either by donor or acceptor impurities or by additional pockets of states, the Fermi surface has the shape of a tube surrounding the nodal line, as depicted in Fig. 1(a). For realistic doping levels, the radius of the tube (the Fermi momentum) is significantly smaller than the characteristic size of the nodal line, which is typically of order of the inverse lattice spacing.

We also assume that the dominant source of momentum scattering for quasiparticles is provided by Coulomb impurities, as is typical for semiconductors and semimetals. Due to the long-range nature of the potential of these impurities, they provide only small-momentum scattering relative to the diameter of the nodal line, so that the curvature of the nodal line may be neglected in each scattering event. Scattering processes between opposite sides of the nodal line can also be neglected.

The Hamiltonian for a quasiparticle near a short straight segment of the nodal line is given by²

$$\hat{\mathcal{H}}_0 = v(\hat{\sigma}_x k_x + \hat{\sigma}_y k_y) + \xi(k_z) + e\phi(\mathbf{r}), \quad (1)$$

where k_x and k_y are the transverse momentum components (hereinafter $\hbar = 1$); $\hat{\sigma}_x$ and $\hat{\sigma}_y$ are Pauli matrices in the space of a spin-1/2 degree of freedom (pseudospin space); v is the velocity of transverse motion, which for simplicity is assumed to be the same in the x and y directions throughout this paper; $\xi(k_z)$ is the contribution of the longitudinal motion to the kinetic energy; $\phi(\mathbf{r})$ is the electric potential created by charged impurities screened by electrons.

²In principle, the quasiparticle dispersion may have a more complicated form than that of Eq. (1), involving additional spin or valley degrees of freedom. Such additional degrees of freedom would affect only numerical coefficients in our results for the conductivity, so long as the dispersion is linear near the nodal line.

¹See Ref. [36] for a review.

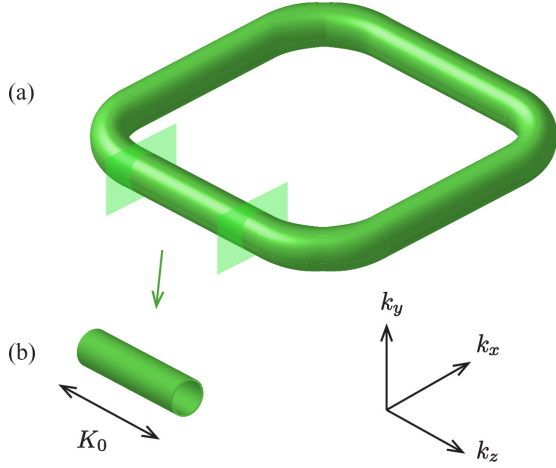


FIG. 1. Fermi surface (FS) in a doped NLS. (a) FS for a closed nodal line. (b) A straight segment of the FS. For a long-range-correlated disorder potential, characteristic of Coulomb impurities, the momentum scattering along the nodal line is small, and the line may be approximated by a chain of straight segments. The total conductivity is given by the sum of the segment contributions.

For the small quasiparticle energies under consideration, the longitudinal quasiparticle velocity may be estimated as $v_z \simeq vk_z/p_0$, and it is strongly suppressed compared to the transverse velocity v , where p_0 is the local radius of curvature of the nodal line (in momentum space). As a result, the quasiparticle dynamics on sufficiently short length scales is effectively 2D and is confined to the plane perpendicular to the segment of the nodal line under consideration.

The strength of the Coulomb interaction in an NLS may be characterized by the effective fine structure constant $\alpha = \frac{e^2}{\kappa v}$ (in Gaussian units), with κ being the dielectric constant. Usually, $\alpha \lesssim 1$ in semimetals (see, e.g., Refs. [21] and [22] for estimates). In this Rapid Communication, we make the usual weak-interaction assumption, $\alpha \ll 1$, which allows one to use the linear Poisson equation to describe the electrostatic potential $\phi(\mathbf{r})$ created by screened charged impurities:

$$\begin{aligned} \kappa \nabla^2 \phi(\mathbf{r}) + 4\pi e^2 \int \Pi(\mathbf{r}, \mathbf{r}') \phi(\mathbf{r}') d\mathbf{r}' \\ = -4\pi e \sum_j Z_j \delta(\mathbf{r} - \mathbf{r}_j). \end{aligned} \quad (2)$$

Here, \mathbf{r}_j and $Z_j e$ are the location and the charge of the j th impurity (for donors and acceptors $Z_j = \pm 1$, respectively) and $\Pi(\mathbf{r}, \mathbf{r}') = -i \int_{-\infty}^0 \langle [\hat{n}(0, \mathbf{r}), \hat{n}(t', \mathbf{r}')] \rangle dt'$ is the zero-frequency polarization operator, which describes the linear response of the local density of electrons $\hat{n}(\mathbf{r})$ to the electrostatic potential $\phi(\mathbf{r}')$.

Polarization operator. Due to the effectively two-dimensional short-distance dynamics of the quasiparticles, the screening properties of electrons near a short segment of the nodal line are related to those in graphene [23,24], with the contribution to the polarization operator given by that of 2D Dirac electrons multiplied by $gK_{\parallel}/(2\pi)$, where g indicates the spin and valley degeneracy and K_{\parallel} is the length of this segment in momentum space. The full polarization

operator is given by a sum of all such straight-line-segment contributions, since the entire nodal line may be approximated as a chain of straight-line segments.

At low temperature and chemical potential, the polarization operator $\Pi(\mathbf{q})$ is linear in the momentum $|\mathbf{q}|$ for any direction of \mathbf{q} . While the constant of proportionality between $\Pi(\mathbf{q})$ and $|\mathbf{q}|$ for a given direction of $|\mathbf{q}|$ depends in general on the shape of the nodal line,³ below we assume for simplicity that the full polarization operator is isotropic in \mathbf{q} . For sufficiently high chemical potentials μ or temperatures T , $\Pi(\mathbf{q})$ is momentum independent and is determined by the density of states (DoS) at energies $\sim \max(|\mu|, T)$. Thus the behavior of the polarization operator in an NLS in the limits of high and low temperatures may be summarized as

$$\Pi(\mathbf{q}) = \begin{cases} -gCK_{\circ}|\mathbf{q}|/v, & v|\mathbf{q}| \gg T, |\mu|, \\ -gK_{\circ}|\mu|/(4\pi^2v^2), & |\mu| \gg T, v|\mathbf{q}|, \\ -gK_{\circ}T \ln 2/(2\pi^2v^2), & T \gg |\mu|, v|\mathbf{q}|. \end{cases} \quad (3)$$

Here, K_{\circ} is the length of the nodal line and C is a constant of order unity, which accounts for the details of the geometry of the nodal line.

Screened impurity potential. At low temperature and chemical potential, the distance dependence of the screened Coulomb potential in an NLS is qualitatively different from that in conventional metals, dielectrics, or other semimetals. The Fourier transform of the screened interaction is given by $\phi(\mathbf{q}) = \phi_0(\mathbf{q})[1 - \Pi(\mathbf{q})\phi_0(\mathbf{q})]^{-1}$, where $\phi_0(\mathbf{q}) = 4\pi e^2/(\kappa q^2)$ describes the unscreened Coulomb interaction and the polarization operator $\Pi(\mathbf{q})$ is given by Eq. (3). At short distances the interaction is unscreened, $\phi(r) \simeq e^2/(\kappa r)$. At distances of order of

$$r_0 = (\alpha g K_{\circ})^{-1}, \quad (4)$$

the interaction potential crosses over to the unconventional form

$$\phi(r) = \frac{e^2 r_0}{2\pi^2 \kappa C} \frac{1}{r^2}. \quad (5)$$

Finally, at very large distances, exceeding the characteristic wavelength $\max(|\mu|, T)/v$ of the quasiparticles in the conduction (valence) band, the polarization operator is effectively local, $\Pi(\mathbf{r}, \mathbf{r}') \approx -(4\pi e^2 \lambda_{\text{TF}}^2 / \kappa)^{-1} \delta(\mathbf{r} - \mathbf{r}')$, resulting in the exponentially suppressed interaction $\phi(r) \propto \exp(-r/\lambda_{\text{TF}})$. Here we have introduced the Thomas-Fermi (TF) screening length, given by

$$\lambda_{\text{TF}}^{-2} = \begin{cases} (g\alpha/\pi) \cdot K_{\circ}|\mu|/v, & |\mu| \gg T, \\ (2g\alpha/\pi) \ln 2 \cdot K_{\circ}T/v, & T \gg |\mu|. \end{cases} \quad (6)$$

The dependence of the screened interaction on distance is summarised in Fig. 2, assuming low temperature and chemical potential ($|\mu|, T \ll \alpha g v K_{\circ}$).

For high temperatures or chemical potentials, $\max(|\mu|, T) \gg \alpha g v K_{\circ}$, the characteristic quasiparticle wavelength becomes shorter than the distance r_0 , and the

³These constants of proportionality between $\Pi(\mathbf{q})$ and $|\mathbf{q}|$ are calculated for the case of a circular nodal line in Ref. [37].

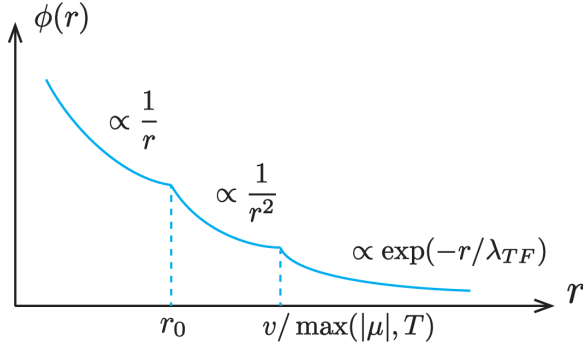


FIG. 2. Screened Coulomb interaction as a function of distance at low temperatures and doping levels.

intermediate regime with $\phi(r) \propto 1/r^2$ (see Fig. 2) vanishes. In this case, the screened electrostatic potential is given by

$$\phi(r) = \frac{e^2}{\kappa r} \exp(-r/\lambda_{TF}) \quad (7)$$

across all distances, as in a conventional metal [25].

Quasiparticle scattering. As mentioned in Introduction, it is possible to approximate the nodal line by a chain of straight-line segments and to consider separately the quasiparticle transport near each segment. Due to the suppressed quasiparticle motion along the nodal line, the transverse conductivity σ_x of a given segment with momentum length K_{\parallel} significantly exceeds its longitudinal conductivity σ_z . The sum of the conductivity from all segments, with their various orientations, is then of order of $\sigma_x K_{\circ}/K_{\parallel}$.

The relaxation of the momentum of quasiparticles with energy ε (transverse momentum ε/v) near a straight segment of the nodal line due to elastic scattering off impurities is characterised by the transport scattering time τ_{tr} . In the Born approximation,

$$\frac{1}{\tau_{tr}(\varepsilon)} = 2\pi n_{imp} \int \frac{d\mathbf{p}}{(2\pi)^3} |\phi(\mathbf{p} - \mathbf{k}) \langle \sigma_{\mathbf{p}} | \sigma_{\mathbf{k}} \rangle|^2 \times (1 - \cos \theta_{\mathbf{k}, \mathbf{p}}) \delta(kv - pv), \quad (8)$$

where n_{imp} is the total concentration of (donor and acceptor) impurities, \mathbf{k} is a momentum with the transverse component ε/v , $\phi(\mathbf{q})$ is the Fourier transform of the impurity potential, and $|\sigma_{\mathbf{p}}\rangle$ is the pseudospin state of a quasiparticle with momentum \mathbf{p} in a given (conduction or valence) band; $|\langle \sigma_{\mathbf{p}} | \sigma_{\mathbf{k}} \rangle|^2 = (1 + \cos \theta_{\mathbf{k}, \mathbf{p}})/2$, with $\theta_{\mathbf{k}, \mathbf{p}}$ being the angle between the transverse components of \mathbf{k} and \mathbf{p} .

Low-doping levels. At low doping, $|\mu| \ll \alpha g v K_{\circ}$, and zero temperature, the Fermi wavelength $\sim \mu/v$ significantly exceeds the length scale r_0 [Eq. (4)]. Thus the scattering of quasiparticles at the Fermi surface is determined by the $\propto 1/r^2$ tail of the impurity potential rather than the $\propto 1/r$ core (see Fig. 2).

Using Eqs. (5) and (8), we find the transport scattering time in this regime to be (see Supplemental Material for details [26])

$$\tau_{tr} = \gamma_{tr} g^2 K_{\circ}^2 / (n_{imp} v), \quad (9)$$

where γ_{tr} is a nonuniversal constant of order unity, which depends on the details of the geometry of the nodal line. We

note that typical scattering events have large scattering angles $\theta_{\mathbf{p}, \mathbf{k}} \sim 1$, and therefore the transport scattering time (9) is of the same order as the typical time τ_0 between collisions (the elastic scattering time).

For weak disorder, such that $\tau_0 \mu \gg 1$, the DoS of quasiparticles at the Fermi energy is weakly affected by impurities, and the conductivity is dominated by the Drude contribution [25,27,28], which takes into account quasiparticle scattering processes not involving quasiparticle interference. The transverse Drude conductivity of the straight nodal-line segment is given by

$$\sigma_x(\mu) = \frac{1}{2} \frac{K_{\parallel}}{2\pi} g e^2 v^2 v_{2D}(\mu) \tau_{tr} = \frac{\gamma_{tr}}{8\pi^2} \frac{g^3 e^2 K_{\circ}^2 K_{\parallel} |\mu|}{n_{imp} v}, \quad (10)$$

where $v_{2D} = \frac{|\mu|}{2\pi v^2}$ is the quasiparticle DoS (per spin per valley) in the transverse 2D plane. As discussed above, the conductivity of the entire NLS is of order (10) with the replacement $K_{\parallel} \rightarrow K_{\circ}$.

Since the concentration of charge carriers depends quadratically on the chemical potential, $n(\mu) \propto \mu^2$, Eq. (10) implies that the quasiparticle mobility $\frac{\sigma_x(\mu)}{en(\mu)} \propto \frac{1}{|\mu|}$ diverges as the chemical potential approaches the nodal line, even for a fixed impurity concentration.

Temperature dependence. In the regime of low doping under consideration ($|\mu| \ll \alpha g v K_{\circ}$), the conductivity strongly depends on temperature when $T \gg |\mu|$ (here, we neglect electron-phonon scattering and the interaction between quasiparticles). In the limit of weak disorder, we find for the conductivity of a straight segment of the nodal line

$$\sigma_x = - \int n_F(\varepsilon) \sigma_x(\varepsilon) d\varepsilon \simeq \frac{\gamma_{tr} \ln 2}{4\pi^2} \frac{g^2 e^2 K_{\circ}^2 K_{\parallel}}{n_{imp} v} T, \quad (T \gg |\mu|), \quad (11)$$

where $n_F(\varepsilon) = 1/[\exp(\varepsilon/T) + 1]$ is the Fermi distribution function and $\sigma_x(\varepsilon)$ is given by Eq. (10). The conductivity of the NLS is described approximately by Eq. (11) with the replacement $K_{\parallel} \rightarrow K_{\circ}$. The linear-in- T dependency of the conductivity comes from thermally activated charge carriers with a linear density of states $\nu(\varepsilon) \propto \varepsilon$ and a constant scattered rate (9).

High-doping regime. When the NLS is so heavily doped that $|\mu| \gg \alpha g v K_{\circ}$, the TF screening radius becomes shorter than r_0 and the screened potential is equivalent to that in a conventional metal [Eq. (7)]. In this regime the transport properties of the NLS are also similar to those of a conventional metal and, in particular, weakly dependent on the temperature. Using Eqs. (7) and (8), we find the transport scattering rate in this regime⁴

$$\frac{1}{\tau_{tr}(\varepsilon)} = \frac{2\pi \alpha^2 v^3 n_{imp}}{\varepsilon^2} \ln \frac{|\varepsilon| \lambda_{TF}}{v}. \quad (12)$$

At such high doping, the impurities typically scatter quasiparticle momenta by small angles $\theta \ll 1$, which leads to a significantly shorter elastic scattering time $\tau_0 = (4\pi \alpha^2 n_{imp} v \lambda_{TF}^2)^{-1}$

⁴This transport scattering is equivalent to the scattering of electrons on the surface of a 3D topological insulator with bulk impurities [38].

(see Ref. [26]). The Drude conductivity of a highly-doped NLS is then given by the segment contribution

$$\sigma_x(\mu) = \frac{gK_{\parallel}e^2|\mu|^3}{8\pi^3\alpha^2v^3n_{\text{imp}}\ln[|\mu|/(\alpha gK_{\circ}v)]}, \quad (13)$$

with K_{\parallel} replaced by a quantity of order K_{\circ} .

Weak localization. For all doping levels, the quasiparticle dynamics on sufficiently short length scales is effectively 2D and is confined to the plane perpendicular to the nodal line. One can therefore expect significant quantum interference effects that are typical of 2D systems [27,29]. In order to estimate the characteristic length scale l_{dim} below which these interference effects are strong, we assume that the quasiparticles have a small longitudinal dispersion $\xi(k_z) = vk_z^2/2p_0$, e.g., due to the curvature of the nodal line (in which case p_0 is the local radius of curvature of the line).

To estimate l_{dim} , let us consider a quasiparticle whose momentum \mathbf{k} at time $t = 0$ lies in the x - y plane. Due to the small dispersion in the z direction and collisions with impurities, such a quasiparticle slowly drifts away from the x - y plane. During each collision with an impurity, the longitudinal velocity of the quasiparticle changes by an amount $\delta v_z \sim \pm vk/K_{\circ}$, where we have assumed that the local radius p_0 of the nodal line is of order K_{\circ} . After a long time $t \gg \tau_0$, the total change in z velocity is of order $\Delta v_z \sim (vk/K_{\circ})\sqrt{t/\tau_0}$, and the quasiparticle travels a distance $\Delta z \sim t\Delta v_z \sim (vk/K_{\circ})\sqrt{t^3/\tau_0}$ in the z direction. When this drift length exceeds the electron wavelength $\sim k^{-1} = v/|\mu|$, the quasiparticle can be considered to have “escaped” its initial 2D plane of motion and no longer participates in the 2D interference effects in this plane. The characteristic time of 2D interference can thus be estimated as $t_{\text{dim}} \sim (v^2K_{\circ}^2\tau_0/\mu^4)^{\frac{1}{3}}$, which corresponds to the length

$$l_{\text{dim}} = (v^4K_{\circ}/\mu^2)^{\frac{1}{3}}\tau_{\text{tr}}^{\frac{1}{2}}\tau_0^{\frac{1}{6}} \quad (14)$$

of diffusion in the initial 2D plane.

Thus, quantum interference effects in an NLS on short distances $L < l_{\text{dim}}$ are equivalent to those of 2D Dirac fermions, such as electrons in graphene in a single valley, which exhibit weak-antilocalization (WAL) corrections to conductivity [30,31]. On larger length scales $L > l_{\text{dim}}$, the classical trajectories of the quasiparticles are essentially 3D and the interference between them is suppressed. Thus the conductivity of the NLS receives a WAL correction

$$\delta\sigma_{WL} = \frac{ge^2K_{\circ}}{(2\pi)^3} \times \begin{cases} \ln[\min(l_{\phi}, l_{\text{dim}})/(v\tau_{\text{tr}})], & B \ll B_0, \\ \tilde{\gamma}_B(\mathbf{n}_B) \cdot \ln[l_B/(v\tau_{\text{tr}})], & B \gg B_0, \end{cases} \quad (15)$$

where $B_0 = \frac{c}{ev\tau_{\text{tr}}\min(l_{\phi}, l_{\text{dim}})}$ is the characteristic value of magnetic field at which the WAL is affected by the field, $\tilde{\gamma}_B(\mathbf{n}_B) < 1$ is a nonuniversal coefficient depending on the geometry of the nodal line and the direction $\mathbf{n}_B = \mathbf{B}/B$ of the magnetic field, l_{ϕ} is the dephasing length, and $l_B = \frac{c}{ev\tau_{\text{tr}}B}$.

The first line in Eq. (15) describes the conventional WAL corrections due to the interference of 2D Dirac fermions [30,31]; the second line describes the partial suppression of WAL by the magnetic field. Because the correction is

dominated by effectively 2D interference effects, the magnetic field \mathbf{B} does not suppress the interference near parts of the nodal line perpendicular to \mathbf{B} (here we neglect the much weaker effect of magnetic field on the motion along the nodal line), and therefore the suppression of the WAL correction by a magnetic field strongly depends on the direction of the field. In particular, if the entire nodal line lies in one plane, as, for example, in ZrSiS [see Fig. 1(a)], the in-plane magnetic field can partially suppress the WAL correction, while the field perpendicular to the plane has no significant effect. We note also that for sufficiently weak disorder ($\mu\tau_{\text{tr}} \gg 1$) the conductivity is dominated by the Drude contribution (10), and the interference correction (15) is negligible.

Summary and discussion. We have studied the conductivity in a weakly disordered NLS with charged impurities. At low temperature and chemical potential, the screened electrostatic interaction is qualitatively different from that in conventional semiconductors and semimetals and includes a broad regime of distances for which $\phi(r) \propto 1/r^2$ (see Fig. 2). Such screening of impurities can potentially be probed using scanning tunneling microscopy,⁵ and it also manifests itself in the dependencies of the conductivity on temperature and doping level.

In particular, a low-doped NLS exhibits divergent quasiparticle mobility $\propto |\mu|^{-1}$ at vanishing chemical potential μ , with conductivity given by Eq. (10). In this regime, the NLS also exhibits strong temperature dependence of the conductivity, $\sigma(T) \propto T$, at $T \gg |\mu|$. At larger doping, the impurities are strongly screened, and the transport properties of the NLS resemble those of a conventional metal.

In all of these regimes, the conductivity of an NLS receives large WAL corrections [Eq. (15)] due to the suppressed motion of the charge carriers along the nodal line, which makes electron dynamics effectively 2D on short scales and thus leads to strong single-particle interference effects.

For presently existing NLSs, which have K_{\circ} of order 1 \AA^{-1} and v of order 10^8 cm/s , the energy scale αgvK_{\circ} is as large as several eV for $\alpha \sim 0.1$. Existing NLS materials are therefore likely to fall in the “low-doping” regime of our analysis. Recent experiments on ZrSiS [32–35], for example, report μ of order 100 meV. In this case, Eq. (10) implies a low-temperature resistivity on the order of tens of $n\Omega \text{ cm}$, assuming a charged impurity concentration of order 10^{19} cm^{-3} (as reported in Ref. [35]). This is consistent with the experimental measurements in Refs. [32,34]. In other NLSs, where the nodal line is not doped by additional pockets of states, it may be possible to achieve lower chemical potentials and significantly higher mobilities. For instance, impurity concentration $n \sim n_{\text{imp}} \sim 10^{18} \text{ cm}^{-3}$ (typical, for example, for Dirac semimetals) will lead to a chemical potential of order

⁵One should keep in mind that for a Coulomb impurity near the surface of a NLS, which could potentially be probed by scanning tunneling microscopy, the Coulomb potential is also affected by the presence of surface states. Such surface states have a finite DOS [13], and therefore contribute to screening. The resulting impurity potential can be calculated straightforwardly, but is beyond the scope of the present work.

10 meV. Equation (10) then implies a huge mobility on the order of $10^7 \text{ cm}^2 \text{ V}^{-1} \text{ s}^{-1}$ and a strong temperature dependence above $T \sim 100 \text{ K}$.

Finally, we note that current experiments correspond to the regime of weak disorder ($\mu\tau_0 \gg 1$), which is assumed throughout this paper and which requires $n_{\text{imp}} \ll g^2 K_o^2 |\mu|/v \sim 10^{21} \text{ cm}^{-3}$. Since there is no localization in systems of effectively-2D Dirac fermions (in the absence of scattering between opposite ends of the nodal line), one can expect that stronger disorder ($n_{\text{imp}} \gg g^2 K_o^2 |\mu|/v$) may lead to a universal minimal conductivity $\sigma \sim e^2 K_o$ in an NLS. However, this regime of strong disorder is left for a future study. Another question that deserves further investigation is the role of the interaction between quasiparticles in transport,

as for sufficiently high temperatures the NLS resistivity will be dominated by the scattering of quasiparticles on each other rather than impurity scattering.

Acknowledgments. we are grateful to M.S. Fuhrer, B. Weber, and especially Ya.I. Rodionov for valuable discussions. S.V.S. was financially supported by AFOSR, NSF QIS, ARO MURI, ARO, ARL CDQI, and NSF PFC at Joint Quantum Institute. B.S. was supported as part of the MIT Center for Excitonics, an Energy Frontier Research Center funded by the US Department of Energy, Office of Science, Basic Energy Sciences under Award no. DE-SC0001088. S.V.S. also acknowledges the hospitality of School of Physics and Astronomy at Monash University and of the MIT Center for Excitonics, where parts of this work were completed.

-
- [1] X. Wan, A. M. Turner, A. Vishwanath, and S. Y. Savrasov, Topological semimetal and Fermi-arc surface states in the electronic structure of pyrochlore iridates, *Phys. Rev. B* **83**, 205101 (2011).
- [2] S.-M. Huang, S.-Y. Xu, I. Belopolski, C.-C. Lee, G. Chang, B. Wang, N. Alidoust, G. Bian, M. Neupane, C. Zhang, S. Jia, A. Bansil, H. Lin, and M. Zahid Hasan, A Weyl Fermion semimetal with surface Fermi arcs in the transition metal monopnictide TaAs class, *Nat. Commun.* **6**, 7373 (2015).
- [3] S.-Y. Xu, I. Belopolski, N. Alidoust, M. Neupane, G. Bian, C. Zhang, R. Sankar, G. Chang, Z. Yuan, C.-C. Lee, S.-M. Huang, H. Zheng, J. Ma, D. S. Sanchez, B. Wang, A. Bansil, F. Chou, P. P. Shibayev, H. Lin, S. Jia, and M. Zahid Hasan, Discovery of a Weyl fermion semimetal and topological Fermi arcs, *Science* **349**, 613 (2015).
- [4] S.-Y. Xu, I. Belopolski, D. S. Sanchez, C. Zhang, G. Chang, C. Guo, G. Bian, Z. Yuan, H. Lu, T.-R. Chang, P. P. Shibayev, M. L. Prokopovych, N. Alidoust, H. Zheng, C.-C. Lee, S.-M. Huang, R. Sankar, F. Chou, C.-H. Hsu, H.-T. Jeng, A. Bansil, T. Neupert, V. N. Strocov, H. Lin, S. Jia, and M. Zahid Hasan, Experimental discovery of a topological Weyl semimetal state in TaP, *Sci. Adv.* **1**, e1501092 (2015).
- [5] S.-Y. Xu, N. Alidoust, I. Belopolski, Z. Yuan, G. Bian, T.-R. Chang, H. Zheng, V. N. Strocov, D. S. Sanchez, G. Chang, C. Zhang, D. Mou, Y. Wu, L. Huang, C.-C. Lee, S.-M. Huang, B. Wang, A. Bansil, H.-T. Jeng, T. Neupert, A. Kaminski, H. Lin, S. Jia, and M. Zahid Hasan, Discovery of a Weyl fermion state with Fermi arcs in niobium arsenide, *Nat. Phys.* **11**, 748 (2015).
- [6] B. Q. Lv, H. M. Weng, B. B. Fu, X. P. Wang, H. Miao, J. Ma, P. Richard, X. C. Huang, L. X. Zhao, G. F. Chen, Z. Fang, X. Dai, T. Qian, and H. Ding, Experimental Discovery of Weyl Semimetal TaAs, *Phys. Rev. X* **5**, 031013 (2015).
- [7] L. M. Schoop, M. N. Ali, C. Straßer, A. Topp, A. Varykhalov, D. Marchenko, V. Duppl, S. S. P. Parkin, B. V. Lotsch, and C. R. Ast, Dirac cone protected by non-symmorphic symmetry and three-dimensional Dirac line node in ZrSiS, *Nat. Commun.* **7**, 11696 (2016).
- [8] G. Bian, T.-R. Chang, R. Sankar, S.-Y. Xu, H. Zheng, T. Neupert, C.-K. Chiu, S.-M. Huang, G. Chang, I. Belopolski, D. S. Sanchez, M. Neupane, N. Alidoust, C. Liu, B. Wang, C.-C. Lee, H.-T. Jeng, C. Zhang, Z. Yuan, S. Jia, A. Bansil, F. Chou, H. Lin, and M. Zahid Hasan, Topological nodal-line fermions in spin-orbit metal PbTaSe₂, *Nat. Commun.* **7**, 10556 (2016).
- [9] T. Kondo, M. Nakayama, R. Chen, J. J. Ishikawa, E.-G. Moon, T. Yamamoto, Y. Ota, W. Malaeb, H. Kanai, Y. Nakashima, Y. Ishida, R. Yoshida, H. Yamamoto, M. Matsunami, S. Kimura, N. Inami, K. Ono, H. Kumigashira, S. Nakatsuji, L. Balents, and S. Shin, Quadratic Fermi node in a 3D strongly correlated semimetal, *Nat. Commun.* **6**, 10042 (2015).
- [10] S. A. Parameswaran, T. Grover, D. A. Abanin, D. A. Pesin, and A. Vishwanath, Probing the Chiral Anomaly with Nonlocal Transport in Three-Dimensional Topological Semimetals, *Phys. Rev. X* **4**, 031035 (2014).
- [11] E. Fradkin, Critical behavior of disordered degenerate semiconductors. i. models, symmetries, and formalism, *Phys. Rev. B* **33**, 3257 (1986).
- [12] D. Takane, Z. Wang, S. Souma, K. Nakayama, C. X. Trang, T. Sato, T. Takahashi, and Y. Ando, Dirac-node arc in the topological line-node semimetal HfSiS, *Phys. Rev. B* **94**, 121108 (2016).
- [13] A. A. Burkov, M. D. Hook, and L. Balents, Topological nodal semimetals, *Phys. Rev. B* **84**, 235126 (2011).
- [14] Y. Kim, B. J. Wieder, C. L. Kane, and A. M. Rappe, Dirac Line Nodes in Inversion-Symmetric Crystals, *Phys. Rev. Lett.* **115**, 036806 (2015).
- [15] L. S. Xie, L. M. Schoop, E. M. Seibel, Q. D. Gibson, W. Xie, and R. J. Cava, A new form of Ca₃P₂ with a ring of Dirac nodes, *APL Mater.* **3**, 083602 (2015).
- [16] C. Fang, Y. Chen, H.-Y. Kee, and L. Fu, Topological nodal line semimetals with and without spin-orbital coupling, *Phys. Rev. B* **92**, 081201(R) (2015).
- [17] L.-Y. Gan, R. Wang, Y. J. Jin, D. B. Ling, J. Z. Zhao, W. P. Xu, J. F. Liu, and H. Xu, Emergence of topological nodal loops in alkaline-earth hexaborides XB₆ (X = Ca, Sr, and Ba) under pressure, *Phys. Chem. Chem. Phys.* **19**, 8210 (2017).
- [18] R. Yu, H. Weng, Z. Fang, X. Dai, and X. Hu, Topological Node-Line Semimetal and Dirac Semimetal State in Antiperovskite Cu₃PdN, *Phys. Rev. Lett.* **115**, 036807 (2015).
- [19] K. Mullen, B. Uchoa, and D. T. Glatzhofer, Line of Dirac Nodes in Hyperhoneycomb Lattices, *Phys. Rev. Lett.* **115**, 026403 (2015).

- [20] G. Bian, T.-R. Chang, H. Zheng, S. Velury, S.-Y. Xu, T. Neupert, C.-K. Chiu, S.-M. Huang, D. S. Sanchez, I. Belopolski, N. Alidoust, P.-J. Chen, G. Chang, A. Bansil, H.-T. Jeng, H. Lin, and M. Z. Hasan, Drumhead surface states and topological nodal-line fermions in TiTaSe_2 , *Phys. Rev. B* **93**, 121113(R) (2016).
- [21] B. Skinner, Coulomb disorder in three-dimensional Dirac systems, *Phys. Rev. B* **90**, 060202(R) (2014).
- [22] Ya. I. Rodionov and S. V. Syzranov, Conductivity of a Weyl semimetal with donor and acceptor impurities, *Phys. Rev. B* **91**, 195107 (2015).
- [23] T. Ando, Screening effect and impurity scattering in monolayer graphene, *J. Phys. Soc. Jpn.* **75**, 074716 (2006).
- [24] E. H. Hwang and S. Das Sarma, Dielectric function, screening, and plasmons in two-dimensional graphene, *Phys. Rev. B* **75**, 205418 (2007).
- [25] A. A. Abrikosov, *Fundamentals of the Theory of Metals* (Elsevier, Oxford, 1988).
- [26] See Supplemental Material at <http://link.aps.org/supplemental/10.1103/PhysRevB.96.161105> for details on the calculation of transport and elastic scattering times.
- [27] K. B. Efetov, *Supersymmetry in Disorder and Chaos* (Cambridge University Press, New York, 1999).
- [28] A. A. Abrikosov, L. P. Gorkov, and I. E. Dzyaloshinski, *Methods of Quantum Field Theory in Statistical Physics* (Dover, New York, 1975).
- [29] V. F. Gantmakher, *Electrons and Disorder in Solids* (Oxford University Press, 2005).
- [30] E. McCann, K. Kechedzhi, V. I. Fal'ko, H. Suzuura, T. Ando, and B. L. Altshuler, Weak-Localization Magnetoresistance and Valley Symmetry in Graphene, *Phys. Rev. Lett.* **97**, 146805 (2006).
- [31] I. L. Aleiner and K. B. Efetov, A Finite-Temperature Phase Transition for Disordered Weakly Interacting Bosons in One Dimension, *Phys. Rev. Lett.* **97**, 236801 (2006).
- [32] M. Neupane, I. Belopolski, M. M. Hosen, D. S. Sanchez, R. Sankar, M. Szlawska, S.-Y. Xu, K. Dimitri, N. Dhakal, P. Maldonado, P. M. Oppeneer, D. Kaczorowski, F. Chou, M. Z. Hasan, and T. Durakiewicz, Observation of topological nodal fermion semimetal phase in ZrSiS , *Phys. Rev. B* **93**, 201104(R) (2016).
- [33] R. Singha, A. K. Pariari, B. Satpati, and P. Mandal, Large non-saturating magnetoresistance and signature of non-degenerate Dirac nodes in ZrSiS , *Proc. Natl. Acad. Sci. USA* **114**, 2468 (2017).
- [34] M. N. Ali, L. M. Schoop, C. Garg, J. M. Lippmann, E. Lara, B. Lotsch, and S. S. P. Parkin, Butterfly magnetoresistance, quasi-2D Dirac Fermi surfaces, and a topological phase transition in ZrSiS , *Sci. Adv.* **2**, e1601742 (2016).
- [35] M. S. Lodge, G. Chang, B. Singh, J. Hellerstedt, M. Edmonds, D. Kaczorowski, M. Mofazzel Hosen, M. Neupane, H. Lin, M. S. Fuhrer, B. Weber, and M. Ishigami, Quasiparticle Interference in the Dirac Line Node Material ZrSiS , [arXiv:1706.05165](https://arxiv.org/abs/1706.05165).
- [36] S. V. Syzranov and L. Radzihovsky, High-dimensional disorder-driven phenomena in Weyl semimetals, semiconductors and related systems, [arXiv:1609.05694](https://arxiv.org/abs/1609.05694).
- [37] Y. Huh, E.-G. Moon, and Y. B. Kim, Long-range Coulomb interaction in nodal-ring semimetals, *Phys. Rev. B* **93**, 035138 (2016).
- [38] B. Skinner, T. Chen, and B. I. Shklovskii, Effects of bulk charged impurities on the bulk and surface transport in three-dimensional topological insulators, *J. Exp. Theor. Phys.* **117**, 579 (2013).